Supporting Information

A Nanocatalyst-Based Assay for Proteins: DNA-Free Ultrasensitive Electrochemical Detection Using Catalytic Reduction of *p*-Nitrophenol by Gold-Nanoparticle Labels

Jagotamoy Das, Md. Abdul Aziz, and Haesik Yang*

Department of Chemistry, Pusan National University, Busan 609-735, Korea

Chemicals. Amine-terminated G4 poly(amidoamine) (PAMAM) dendrimer, ferrocenecarboxaldehyde, 3-phosphonopropionic acid (PPA), sodium borohydride ($NaBH_4$), *p*-nitrophenol (NP), *p*-aminophenol (AP), hydrogen peroxide, and ammonium hydroxide were purchased from Aldrich. Mouse IgG from serum, rabbit anti-mouse IgG, biotinylated goat anti-mouse IgG, goat IgG, (+)-biotin *N*-hydroxy-succinimide ester, streptavidin from *streptomyces avidinii,* human prostate specific antigen (PSA), rabbit anti-PSA, 1-Ethyl-3-[3-(dimethylamino)propyl]carbodiimide hydrochloride (EDC), and gold nanoparticle (10 nm, 0.01% $HAuCl_4$) were purchased from Sigma. Biotinylated anti-human PSA was from R & D systems (www.rndsystems.com). *N*-hydroxysuccinimide (NHS) and polyethylene glycol (PEG, MW = 20,000) were obtained from Fluka. All buffer reagents and other inorganic chemicals were supplied by Sigma, Aldrich, or Fluka, unless otherwise stated. All chemicals were used as received. All aqueous solutions were prepared in doubly distilled water.

The PBS solution consisted of 0.01 M phosphate buffered saline, 0.138 M NaCl and 0.138 M KCl (pH 7.4). The PBSB solution contained all of the ingredients of PBS and additionally 1% (w/v) bovine serum albumin (pH 7.4). The binding buffer (BB) was made by using PBSB and 0.05% (v/v) Tween 20 (pH 7.4). The rinsing buffer (RB) was composed of 50 mM tromethamine (tris), 40 mM HCl, 0.5 M NaCl, 0.05% (w/v) bovine serum albumin, and 0.05% Tween 20 (pH 7.4). The buffer (EB) for the electrochemical experiment was made by 50 mM tris, 10 mM KCl, 1 g/L $MgCl_2$, and 7 mM HCl (pH 9.0).

Preparation of partially ferrocenyl-tethered PAMAM G4 dendrimer. Partially ferrocenyl-tethered PAMAM dendrimer (Fc-D) was synthesized by an imine formation reaction between primary amines of dendrimer and ferrocenecaroxaldehydes, as previously described.[S1,S2] Ferrocenecarboxaldehyde (2.5 mg) was dissolved in 10 mL of methanol, and 1 mL of this solution was diluted to 3 mL by adding methanol, which was then added dropwise to 500 μL of 10% (w/w) G4 PAMAM dendrimer solution containing hydrochloric acid as a catalyst. The reaction mixture was slowly stirred for 2

h. 286 μL of 0.1 M $NaBH_4$ in methanol was slowly added, and the resulting solution was stirred for 1 h to reduce immine. The reaction product was purified by liphophilic gel permeation chromatography (Sephadex LH-20, Pharmacia) using methanol as an eluent. On the basis of NMR and UV/Vis spectra,[S1] the extent of primary amine modification was estimated to be 0.5%.

Preparation of IgG-nanocatalyst conjugate. An anti-mouse IgG-nanocatalyst conjugate was synthesized by following the published protocol.[S3,S4] Briefly, the optimum amount of IgG for stabilization of a known volume of a gold colloid solution was estimated as follows. A serial dilution of IgG in PBS was prepared to a volume of 50 μL in a small glass vial, and 0.5 mL of colloidal gold solution was added rapidly. After 1 min, 0.5 mL of 10% NaCl in distilled water was added, and the mixture was allowed to stand for 5 min. The stability of gold sol was monitored by measuring absorbance at 520 nm. The mixture giving highest absorbance was stable, and the amount of IgG present in that mixture (40.3 μg) was the stabilizing amount of 0.5 mL of gold colloids. A stabilizing amount of antibody plus an additional 10% (1770 μg) was mixed well with the appropriate volume (20 mL) of colloidal gold. After 1 min, 500 μL of 1% PEG was added. The reaction mixture was stirred for an additional 5 min. To remove excess IgG, the crude IgG-nanocatalyst conjugate was centrifuged at 20,000 g for more than 2 h at 4 ºC. The colorless supernatant was carefully pipetted off, and the sedimented IgG-nanoctalyst conjugate was resuspended to a final volume of 20 mL with PBS containing 833 μL of 1% PEG, and stored at 4 ^{0}C.

Similarly, a stabilizing amount of rabbit anti-PSA plus an additional 10% was mixed well to 564 μL of gold colloids. After removing excess IgG by centrifugation at 20,000 g for more than 2 h at 4 ºC, the sedimented IgG-nanocatalyst conjugate was resuspended to a final volume of 5 mL with PBS containing 150 μL of 1% PEG, and stored at 4 ºC.

Construction of electrochemical immunosensors. Indium-tin oxide (ITO) electrodes were obtained from Geomatec (www.geomatec.co.jp). ITO electrodes were cleaned with ethanol, acetone, 2-propanol, and water successively, and dried at 60 ºC. The cleaned substrates were pretreated in the mixture of 5:1:1 H_2O/H_2O_2 (30%)/NH_4OH (30%) at 70 ºC for 1.5 h to ensure the presence of active hydroxyl group on surface. Then, the substrates were washed with copious amount of water and dried. The pretreated ITO electrodes were immersed in a 0.1 mM PPA aqueous solution for 36 h at room temperature for PPA monolayer formation. The substrates were then washed with distilled water. The carboxylic groups were activated by immersion of the electrodes into a mixed solution of 50 mM EDC and 25 mM NHS for 2 h, and the Fc-D solution

(100 μM) was spotted onto the activated electrodes and left to incubate for 2 h. Nonspecifically adsorbed Fc-D was removed by rinsing twice with RB. Biotin was attached to the Fc-D modified electrode by immerging it for 2 h in a solution containing 1.5 mg/mL (+)-biotin *N*-hydroxy-succinimide ester, and then the electrode was washed with methanol and water. The biotin-modified Fc-D electrodes were immerged in PBS containing 100 μg/mL streptavidin for 30 min and washed twice with water. The streptavidin-coated electrodes were incubated in BB for 30 min to minimize nonspecific binding. After washing with RB, the electrodes were immersed for 30 minutes in PBSB containing 100 μg/mL biotinylated goat anti-mouse IgG, and washed with RB. Then, the substrates were incubated for 30 minutes in PBSB containing variable concentrations of mouse IgG. After rinsing with RB, the resulting assembly was immersed in PBS containing anti-mouse IgG-nanocatalyst conjugate, followed by washing with PBS. Concentrations of anti-mouse IgG and gold nanocatalyst of the IgG-nanocatalyst conjugate solution were ca. 80.5 μg/mL and 6.06 nM, respectively.

Similarly, we constructed PSA immunosensor using biotinyalted anti-PSA (1 μg/mL), PSA, and anti-PSA IgG-nanocatalyst conjugate instead of biotinylated anti-mouse IgG (100 μg/mL), mouse IgG, and anti-mouse IgG-nanocatalyst conjugate. Concentrations of anti-PSA IgG and gold nanocatalyst of the anti-PSA-nanocatalyst conjugate solution were ca. 9.08 μg/mL and 0.68 nM respectively.

The electrochemical experiments were performed using a CHI617b (CH instruments, Inc) and a CHI708c (CH instruments, Inc). The electrochemical cell consisted of the immunosensing working electrode, a Pt wire counter electrode, and a Ag/AgCl reference electrode. The cell was filled with EB containing a mixture of 5 mM NP and 5 mM $NaBH_4$. $NaBH_4$ solution was prepared freshly each time.

Nanocatalyst kinetics. In the standard quartz cuvette with a 1-cm pathlength, 50 mM tris, IgG-nanocatalyst conjugate, and excess amount of $NaBH_4$ (more than 50 times concentration of NP) were taken. After 10 min, NP was added and mixed well. This 10 min satisfies the induction time[S5,S6] of gold nanocatalyst and the time for reaching the mixture to the reaction temperature (i.e., 20 ºC). Time-course spectra were taken at fixed wavelength of 400 nm. The absorption spectra were recorded with a UV-visible spectrophotometer (Shimadzu UV-1650 PC).

The concentration of gold nanocatalyst was estimated by assuming that a gold nanoparticle is an ideal ball tightly packed with gold atoms.[S7]

Previous studies show[S5,S6,S8] that in the absence of any catalyst, the peak due to NP at 400 nm remains unaltered even for a couple of days. Addition and proper mixing of nanocatalyst to the reaction mixture cause fading and ultimate bleaching of the yellow color of NP. As the amount of nanocatalyst is very small, it hardly interfere the

absorption spectra of NP. The reduction can be visualized by the disappearance of the NP peak at 400 nm with the concomitant appearance of the new peak at 300 nm that is attributed to AP. Since the concentration of $NaBH_4$ is very high, it remains excess during the reaction.

Figures S1a and S2a show the decrease of absorption with time at 400 nm owing to the reduction of NP. Figures S1b and S2b were obtained from the data obtained in Figures S1a and S2a after converting absorbance into concentration by dividing with extinction coefficient. The Figures S1b and S2b represent the Michaelis-Menten mechanism. In case of enzyme, it is essential to use the initial rate of reaction, because the product of an enzymatic reaction affects the rate of reaction. However, in case of gold nanocatalyst, NP reduction is not reversible, and the product (AP) does not affect the rate of NP reduction. Therefore, the rate at any concentration can be considered as the initial rate for respective concentration. From the fitted data, $V_{\max}$ and K_M were obtained. Turnover number (k_{cat}) and catalytic efficiency (k_{cat}/K_M) of gold nanocatalyst are $1.6 \pm 0.5 \times 10^4$ s^{-1} and $6.9 \pm 0.8 \times 10^7$ M^{-1} s^{-1}, respectively. k_{cat} and k_{cat}/K_M of IgG-nanocatalyst conjugate are $1.5 \pm 0.7 \times 10^3$ s^{-1} and $1.9 \pm 0.4 \times 10^7$ M^{-1} s^{-1}, respectively. The high reaction rate is due partially to the large number of catalytic sites per nanocatalyst. The k_{cat} and k_{cat}/K_M values show that there is no significant decrease in the catalytic activity of gold nanocatalyst even after IgG conjugation to gold nanocatalyst. We believe that this is due to the easy access of small NP molecules to the gold-nanocatalyst surface through pinholes of IgG-nanocatalyst conjugate.

$NaBH_4$ oxidation on different electrodes. $NaBH_4$ is electrochemically oxidized on commonly employed platinum, gold, and glassy carbon electrodes at potential where AP is oxidized (Figure S3), which inflicts high background current. $NaBH_4$ oxidation current on these electrodes are very high, these are ca. 8301, 5245 and 274 $\mu A/cm^2$ (highest values of Figure S3 data were taken) on platinum, gold, and glassy carbon electrodes, respectively. On the contrary, the electron transfer kinetics of $NaBH_4$ on ITO electrodes is so slow that the oxidation current of $NaBH_4$ on ITO electrodes (Figure S3b) is much lower (2.5 $\mu A/cm^2$) than those on the common electrodes.

Control experiment. As an additional control to test nonspecific binding, we examined the effect of replacing mouse IgG with goat IgG (Figure S4). In this case, the peak current was very small and similar to that in the absence of mouse IgG. The small difference in two peak currents indicates that the nonspecific binding of goat IgG is negligible.

Dependance of cyclic voltammograms on the concentration of mouse IgG and PSA.

Figure S5 shows the dependence of peak current on concentration of mouse IgG, and Figure S6 shows the dependence of peak current on concentration of PSA.

The peak current without both mouse IgG and IgG-nanocatalyst conjugate is similar to that in the absence of anti-PSA IgG (Figure S6a). Compared to mouse-IgG case (ii and iii Figure 2b), the peak-current difference is smaller. The smaller difference means lower nonspecific binding of anti-PSA IgG-nanocatalyst conjugate. It seems that the lower concentration of anti-PSA IgG in IgG-nanocatalyst conjugate solution (9.08 μg/mL) than that of anti-mouse IgG (80.5 μg/mL) is responsible for lower nonspecific binding of anti-PSA IgG-nanocatalyst conjugate.

References

S1. Yoon, H.C.; Hong, M.-Y.; Kim, H.-S. *Anal. Chem.* **2000**, *72*, 4420−4427.
S2. Yoon, H.C.; Hong, M.-Y.; Kim, H.-S. *Anal. Biochem.* **2000**, *282*, 121−128.
S3. Roth. J. *J. Histochem. Cytochem.* **1982**, 30, 691−696.
S4. Hermanson, G. T. *Bioconjugate Techniques*, 1st ed.; Academic Press: San Diego, 1996; pp 593−601.
S5. Pradhan, N.; Pal, A.; Pal, T. *Colloids Surf. A: Physicochem. Eng. Aspects* **2002**, *196*, 247−257.
S6. Mei, Y. et al. *Langmuir* **2005**, *21*, 12229−12234.
S7. Zhang, J. et al. *J. Am. Chem. Soc.* **2006**, *128*, 8575−8580.
S8. Kunio, E.; Ryoko, I.; Tomokazu, Y. *Langmuir* **2004**, *20*, 237−243.

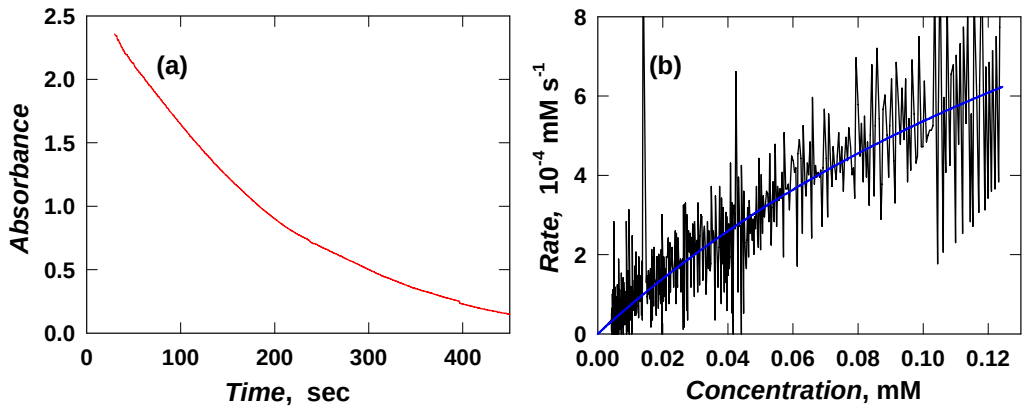

Figure S1. (a) Time-course UV-visible spectrum for the reduction of NP by gold nanocatalyst at 400 nm. (b) Michaelis-Menten plot for the reduction of NP by gold nanocatalyst. Conditions, [NP] = 0.2 mM; [gold nanocatalyst] = 126 pM; [$NaBH_4$] = 10 mM.

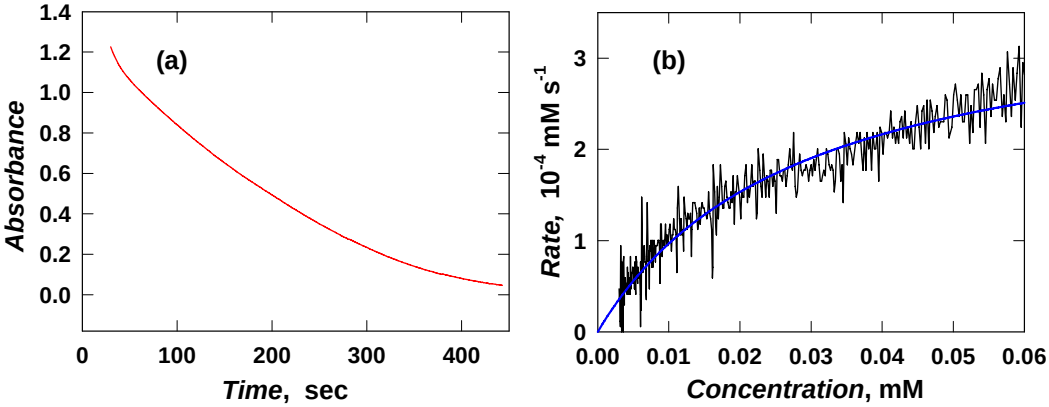

Figure S2. (a) Time-course UV-visible spectrum for the reduction of NP by IgG-nanocatalyst conjugate at 400 nm. (b) Michaelis-Menten plot for the reduction of NP by IgG-nanocatalyst conjugate. Conditions, [NP] = 0.1 mM; [IgG-nanocatalyst conjugate] = 505 pM; [$NaBH_4$] = 10 mM.

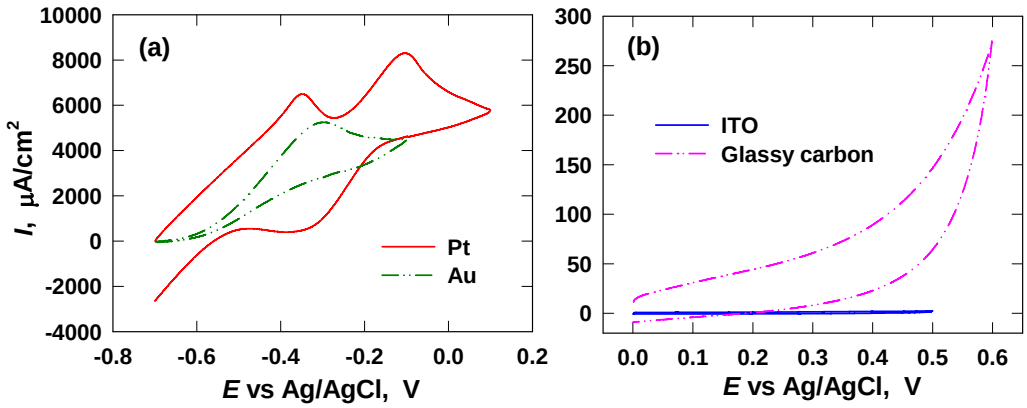

Figure S3. Electrochemical oxidation of $NaBH_4$ on four different electrodes. Cyclic voltammograms were obtained with (a) Pt, Au, (b) glassy carbon, and ITO electrodes in a Tris buffer solution (pH 9.0) containing 5 mM $NaBH_4$ at a scan rate of 50 mV/s.

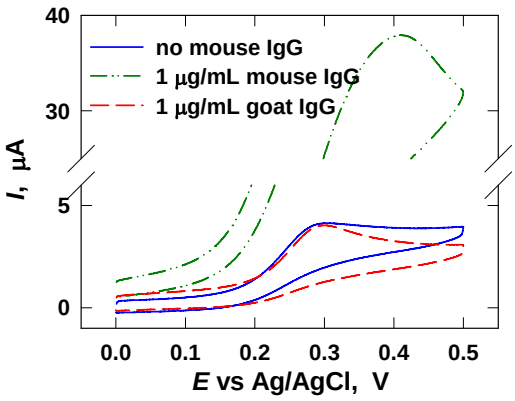

Figure S4. Cyclic voltammograms of immunosensing electrodes obtained after incubating for 10 min in a Tris buffer solution containing 5 mM NP and 5 mM $NaBH_4$ at a scan rate of 50 mV/s. Before this measurement, the electrodes were incubated with no mouse IgG, 1 μg/mL mouse IgG, or 1 μg/mL goat IgG (30 min) and then with anti-mouse IgG-nanocatalyst conjugate (30 min).

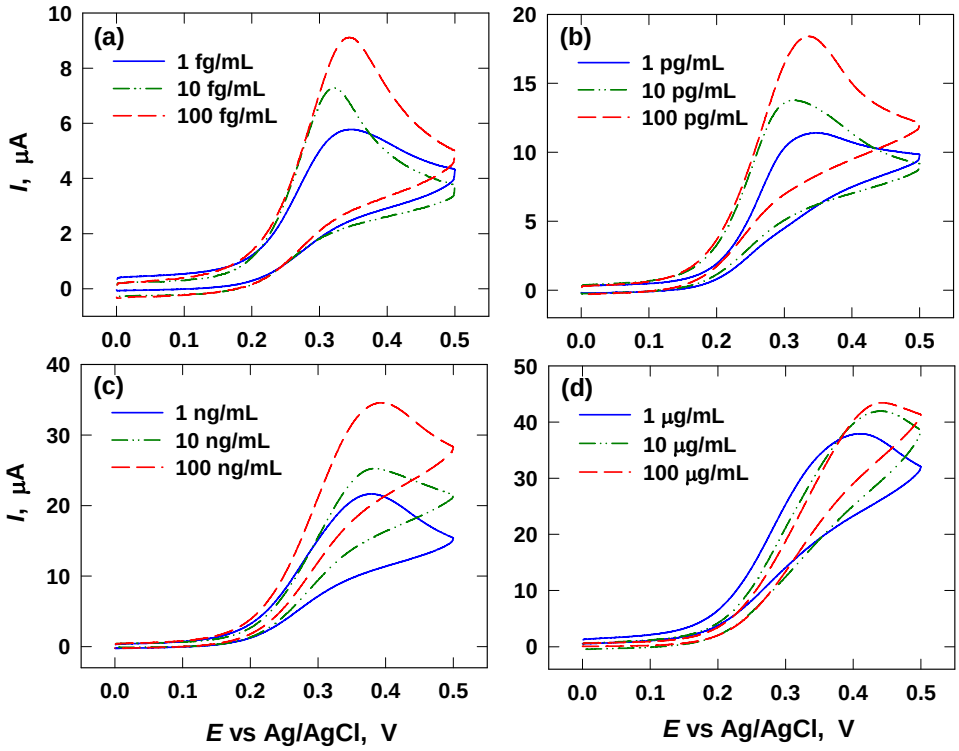

Figure S5. Dependence of cyclic voltammograms on the concentration of mouse IgG. The cyclic voltammograms were obtained after incubating for 10 min in a Tris buffer solution containing 5 mM NP and 5 mM $NaBH_4$ at a scan rate of 50 mV/s.

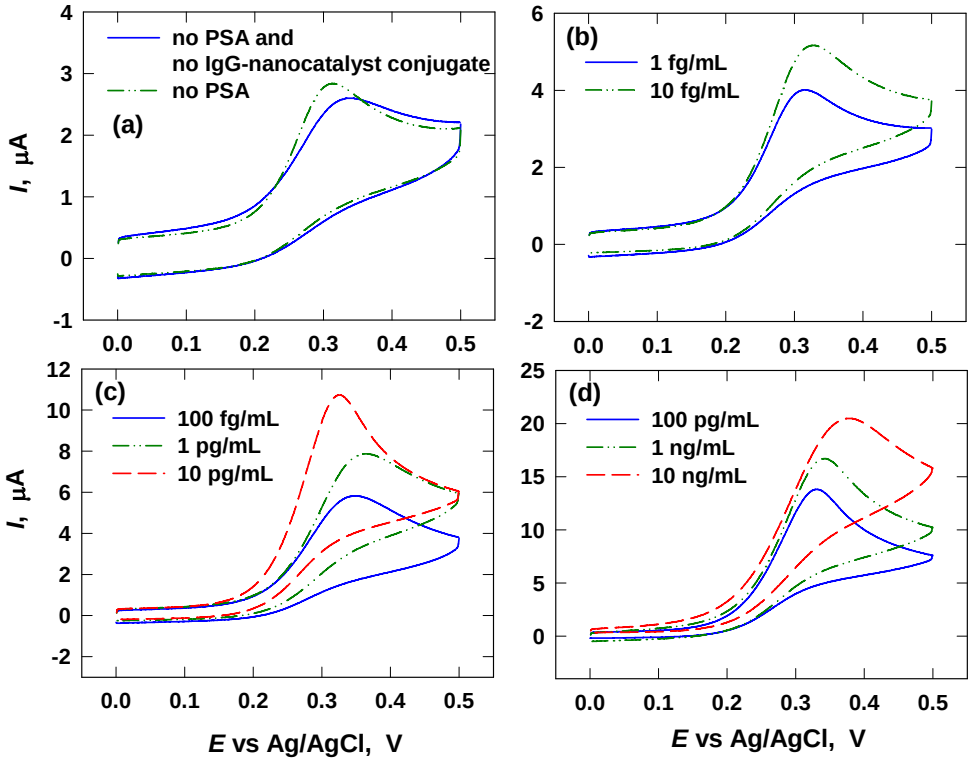

Figure S6. Dependence of cyclic voltammograms on the concentration of PSA. The cyclic voltammograms were obtained after incubating for 10 min in a Tris buffer solution containing 5 mM NP and 5 mM $NaBH_4$ at a scan rate of 50 mV/s.